Earth Planets Space, **56**, 249–258, 2004

Atmospheric density and pressure inferred from the meteor diffusion coefficient and airglow O_2b temperature in the MLT region

H. Takahashi[1], T. Nakamura[2], K. Shiokawa[3], T. Tsuda[2], L. M. Lima[1], and D. Gobbi[1]

[1]*Instituto Nacional de Pesquisas Espaciais, 12245-970 São José dos Campos, SP, Brazil*
[2]*Radio Science Center for Space and Atmosphere, Kyoto University, Uji, Kyoto 611, Japan,*
[3]*Solar-Terrestrial Environment Laboratory, Nagoya University, Toyokawa 442-8507, Japan*

(Received September 15, 2003; Revised February 18, 2004; Accepted February 19, 2004)

Atmospheric density and pressure in the upper mesosphere-lower thermosphere (MLT) region, around 90 km, are inferred from the meteor trail ambipolar diffusion coefficients, D, and simultaneously observed airglow O_2b rotational temperatures. For the present study simultaneous observation data from the meteor radar and SATI imaging spectrometer taken at Shigaraki MU radar observatory (34.9°N, 136.1°E) were used. From the 18 winter nights of data, it is observed that in most of the cases nocturnal variation of the O_2 temperature has a good correlation with D at 90 to 92 km. The inferred densities at 90 km showed a negative correlation with temperature variation, suggesting a constant pressure process. The O_2 emission intensity shows a good correlation with the temperature, and negative correlation with the density variation. The OH rotational temperature and D at 87 km also showed similar results to the case of the O_2 temperature.

Key words: Airglow, meteor trail, temperature, density, pressure.

1. Introduction

The earth's upper mesosphere and lower thermosphere (MLT) is a photochemically and dynamically very active region. Atomic oxygen recombination process produces a series of oxygen-hydrogen reaction chain, releasing kinetic and chemical energy, and airglow emissions. Tidal and gravity waves propagated from the lower atmosphere start breaking and having an important role in vertical transport of atomic oxygen. The MLT region is, therefore, a good place to investigate energy balance and coupling process between the middle and upper atmosphere. However, measurements of fundamental atmospheric parameters, i.e., density, temperature, pressure, and minor constituents in this region are not easy. Simultaneous measurements of these parameters are much more limited. When we study spatial and temporal variation of the airglow emission rates, it is essential to obtain information of these atmospheric parameters. Airglow climatology making use of recent atmospheric model and satellite data has been carried out with a some success (Makhlouf *et al*., 1998, Zhang *et al*., 2001). Lack of groundbased observation data, however, makes it difficult to advance the discussion further.

Atmospheric temperature in the MLT region has been observed by OH rotational temperature (Meinel, 1950; Bittner *et al*., 2002). Molecular oxygen emission, O_2b(0,1) band at 866 nm, was also used to derive its rotational temperature (Wiens *et al*., 1991). Lidar techniques made it possible to observe the height profile of the temperature from 80 to 100 km, using sodium atom resonance scattering (Yu and She, 1995). Meteor radar has also been used to retrieve temperature. Meteor trail ambipolar diffusion coefficient is depending on the local atmospheric temperature and pressure. Applying a Boussinesq approximation between the temperature and density perturbation, Tsutsumi *et al*. (1994) showed temperature as a function of the meteor diffusion coefficient. Hocking *et al*. (1997) presented seasonal variation of $T/P^{1/2}$ as a parameter directly related to the diffusion coefficient. Hocking (1999) further developed an algorithm to determine absolute values of the temperatures. In the algorithm he only assumed a temperature gradient in the mesopause heights. But the temperature gradient should vary with time, season and latitude. Therefore this technique requires a temperature gradient model for different season and location, or comparative study with the other technique to find out the temperature gradient.

Atmospheric density and pressure were retrieved by using meteor trail diffusivity and OH rotational temperature by Takahashi *et al*. (2002). They found that the temperature and density in the emission layer at around 87 km are anti-correlated, and the OH emission rates are well correlated with the temperature, but not with the density. The results are somewhat in contradiction to our present knowledge about the airglow OH emission process. Vibrationally excited OH is mainly produced by a hydrogen-ozone reaction, $H + O_3 \rightarrow OH(v) + O_2$. The ozone is produced by 3 body oxygen recombination process, $O + O_2 + M \rightarrow O_3 + M$, where M is a third element (N_2 and O_2), and is mainly lost by the reaction with hydrogen. Under photochemical equilibrium condition of the ozone, therefore, the OH emission rate is proportional to the ozone production rate. The ozone production is, in turn, approximately proportional to the neutral density (square) and the reaction rate, which is a function

of $(1/T)^{2.3}$ (for example, Makhlouf *et al.*, 1995). This indicates that the emission rates should be negatively correlated with the temperature. However, what we observed contradicts this simple assumption. This argument suggested to further investigate the relation of the airglow emission rates compared to the density and temperature variations.

Between 70 and 120 km of altitude, most meteoroids (with diameter from a few microns to a few mm) are ablated forming ion-electron trails. Meteor radar (and MF radar, too) illuminates the trails by HF radio waves and measures their diffusion decay time and Doppler shift of their frequency. The former provides a diffusion coefficient and the latter gives a trail radial drift velocity. The ion trail diffusion is mainly through ion ambipolar diffusion and eddy diffusion processes. In underdense trail condition (in the case when the forces between the ions and molecules are long-range), the diffusion is mainly through ambipolar diffusion. Jones (1995) mentioned that the coefficient, D, should be related to the ambient gas kinetic temperature T and the atmospheric density, ρ, through the relation,

$$D \propto T/\rho \tag{1}$$

According to Chilson *et al.* (1996), the ionic diffusion coefficient Di, in a dilute system of ions and electrons in a neutral gas, is given through the Einstein relation,

$$Di = (kT/e)(T/273.16)(1.013 \times 10^5/P)Ko, \tag{2}$$

where k is the Boltzmann constant, e is the electronic charge, 1.6×10^{-19} C, P is pressure in Pascal and Ko is the ion mobility in m^2s^{-1}. The ambipolar diffusion coefficient is related to the ion diffusion coefficient,

$$D = Di(1 + Te/Ti), \tag{3}$$

where Te and Ti are the electron and ion temperature, respectively. If we assume that Ti equals to Te through collisional thermal equilibrium below 100 km. (3) becomes

$$D = 2Di \tag{4}$$

Therefore, using (2), D can be presented as,

$$D = 6.39 \times 10^{-2}(T^2/P)Ko. \tag{5}$$

The ion mobility in the meteor trail, is $Ko = 2.5 \times 10^{-4}$ m^2s^{-1} assuming that the main ions are metallic (M^+) and the ambient neutral species are N_2 (Chilson *et al.*, 1996; Hocking, 1997). From Eq. (5) atmospheric pressure can be determined if we get information about the temperature by the other means.

$$P = 1.60 \times 10^{-5}(T^2/D) \tag{6}$$

The atmospheric number density, $[n]$ in cm^{-3}, can be calculated using the ideal gas state equation, $P = [n]kT$ and (6);

$$[n] = 1.159 \times 10^{12}(T/D) \tag{7}$$

In the present work the O_2 and OH rotational temperatures, and D are used to calculate the number density and pressure. The D can be obtained as a function of height and time, $D(z, t)$, but the two emissions are from different altitudes and their peak height would change with time. From airglow rocket observations, it is well known that the O_2b emission peak height is located at around 94 ± 2 km (Greer *et al.*, 1986) and the OH emission is located at 87 ± 2 km (Baker and Stair, 1988). Recent satellite measurements by UARS/WINDII (Upper atmosphere Research Satellite/Wind Imaging Interferometer) reveal that the OH emission peak height should vary more than 2 km, depending on the local time, season and latitude (Zhang *et al.*, 2001). As a first step we choose the O_2 temperature (TO_2) to be from 94 km and the OH temperature (TOH) from 87 km. As mentioned later, however, the assumption of the O_2b emission height gave disagreement with our present correlation analysis between D and TO_2. Rather we feel that the emission height should be around 90 km. Our discussion is focused first on the cross-correlation between the D and TO_2 and TOH with different height of D, and then on calculation of the atmospheric density and pressure. The inferred density and pressure variations were compared with variations of the temperature and the airglow emission rates.

2. Observation

2.1 MU radar

The Middle and Upper atmosphere (MU) radar is a large atmospheric radar, observing neutral wind and turbulence in the mesosphere, stratosphere and troposphere (as an MST radar), and incoherent scatter from the ionosphere (as an IS radar). The system is a monostatic pulsed Doppler radar. The main characteristics are summarized in Table 1. In meteor mode the transmission beam pattern is distorted so as to provide maximum radiation at zenith angles of 30–40° with an isotropic beam pattern in the azimuth direction, in order to increase the meteor echo number. Reception is handled by an array of 4 independent Yagi antennas out of 475 Yagi's in the triangular arrays with a spacing of 0.697 wavelength, so as to measure the echo arrival direction accurately (Nakamura *et al.*, 1997). Although the largest triangle out of 4 antennas is useful in obtaining a better precision in the direction measurement and the additional antenna act to minimize the ambiguity in direction, there are still some ambiguity for the meteors with an elevation angle smaller than 33.5 degree in a similar way as discussed in Nakamura *et al.* (1991). Therefore, these ambiguous meteors are discarded and not used for the further analysis. In this way meteor echoes are observed in the 75–100 km altitude range over a 200 km diameter horizontal area at 90 km. Details of the transmitting and receiving antennas and data processing procedure have been presented by Nakamura *et al.* (1991). In the meteor radar mode of the MU radar, horizontal wind velocities, N-S and E-W components and the meteor trail ambipolar diffusion coefficient are measured, as a function of height from 75 to 100 km, with a height resolution of 1 km. The time integration used to determine the diffusion coefficient for the present work was about 30 minutes.

2.2 SATI O_2b(0,1) and OH(6,2) band measurements

The O_2b(0,1) band P branch spectra at 867 nm and OH(6,2) Q branch spectra at 836 nm were observed by a spectral airglow temperature imager (SATI). The imager characteristics have been published elsewhere (Wiens *et al.*

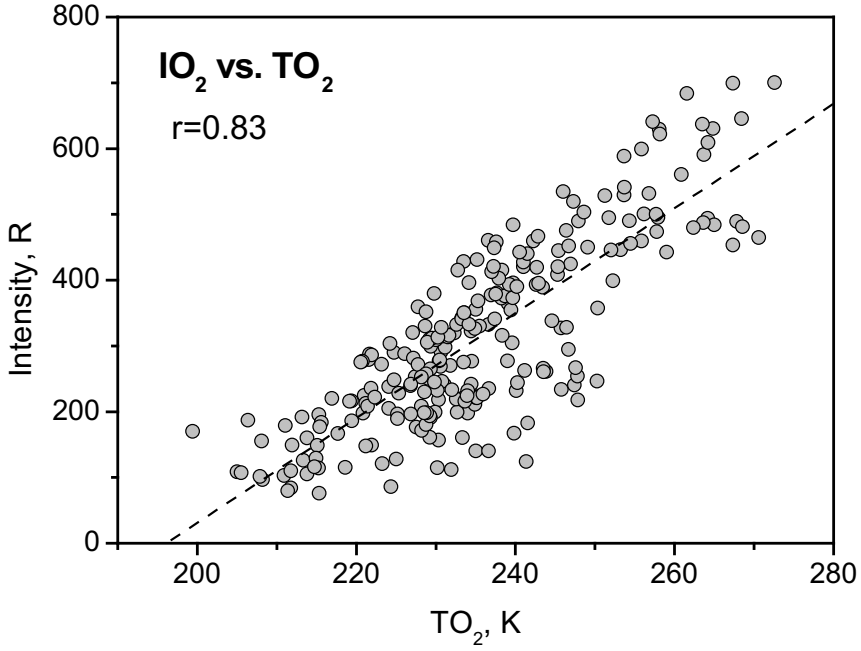

Fig. 1. Correlation between the observed O_2b(0,1) band intensity and O_2 rotational temperature. Each plot corresponds to a half-hourly averaged value. Data base: see Table 2.

Table 1. MU radar characteristics (meteor radar mode).

Item	Characteristics
Observatory	Shigaraki (34.85 N, 136.1 E)
Antenna system	circular array of 475 crossed Yagi
Operational frequency	46.5 MHz
Bandwidth	1.65 MHz
Beam width	3.6 deg.
Transmitter	Peak 1 MW, average 50 kW
Aperture	8330 m^2, 103 m in diameter
Beam angle	30–40 degree from zenith
Time resolution	0.5 hour
Height resolution	1 km

Table 2. Database of the meteor ambipolar diffusion coefficients, O_2b(0,1), and OH(6,2) temperatures used in the present work.

	No. of night	O_2b(0,1) data points	OH(6,2) data points
1998	7	104	-
1999	6	79	-
2000	5	64	64

1997). SATI makes an image of spectral lines (interference fringes) on a CCD camera, employing a technique of spatial spectral scanning. The rotational temperatures of the O_2 and OH are calculated from the line intensities of the rings and the band intensities were calculated from the integrated intensities.

Observation of the O_2 and OH rotational temperature using SATI has been carried out since 1997 as a part of the Optical Mesosphere Thermosphere Imagers system (OMTIs) of Nagoya University (Shiokawa *et al.*, 1999). Two band spectra are measured alternatively by changing the filter with an exposure of 2 minutes. The time resolution of the O_2 and OH temperature is, therefore, 4 minutes. SATI has an annular field of view in the sky, with a radius of $30 \pm 3.5^\circ$ zenith angle centred on the zenith. The temperature and intensity of each emission are obtained for 12 azimuthal sectors in the sky around the zenith. In the present work, azimuthally averaged values are used to compare with the meteor radar measurement carried out at the same place. Data processing to calculate the O_2 and OH rotational temperature has been discussed in Wiens *et al.* (1997).

3. Results

Simultaneous measurements of SATI O_2 airglow and MU radar meteor wind were concentrated during the winter months from November to January from 1998 to 2000. In Table 2 the database is summarized. A total of 18 nights, 247 half-hourly mean values are used in the present analysis. The OH temperature data were also available but only in 2000. Since the data set is different in the two emissions, the present work concentrates on the analysis of the O_2 emission and comparison of the two emissions will be discussed in the later section. In general there is a good correlation between the O_2 emission rate, IO_2, and its rotational temperature TO_2, not only for short term (nocturnal) variation but also for day to day variation. In Fig. 1 the half-hourly means of IO_2 and TO_2 are plotted. A high correlation coefficient, $r = 0.82$, indicates a close correlation between the two parameters. It is interesting to note that there is a clear upper limit of the emission rates for the temperature range from 210 to 260 K. No such limit can be seen for the lower limit.

The meteor trail ambipolar diffusion coefficient D is a function of height, increasing exponentially with height. In Fig. 2 all of the data points of $D(z, t)$ with a half hour aver-

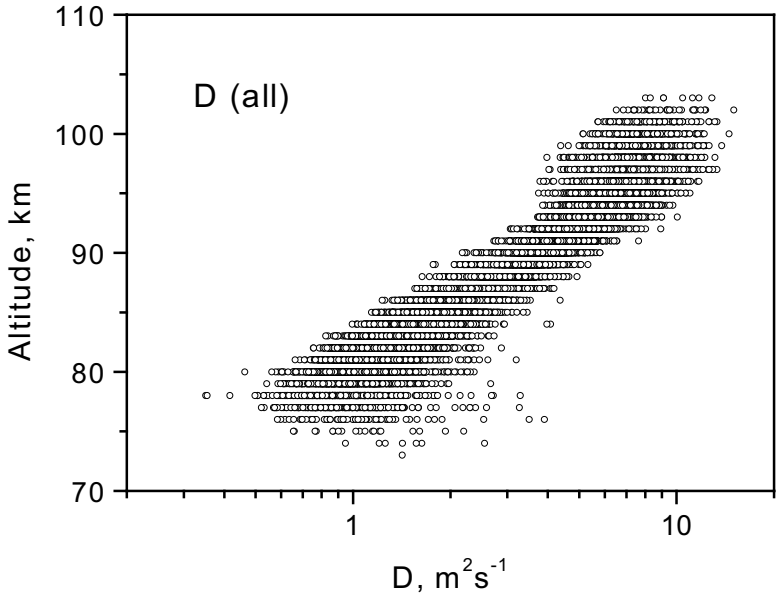

Fig. 2. Meteor trail ambiploar diffusion coefficient, $D(z, t)$, as a function of altitude observed at Shigaraki during the period of 1998 and 2000 (Database: see Table 2).

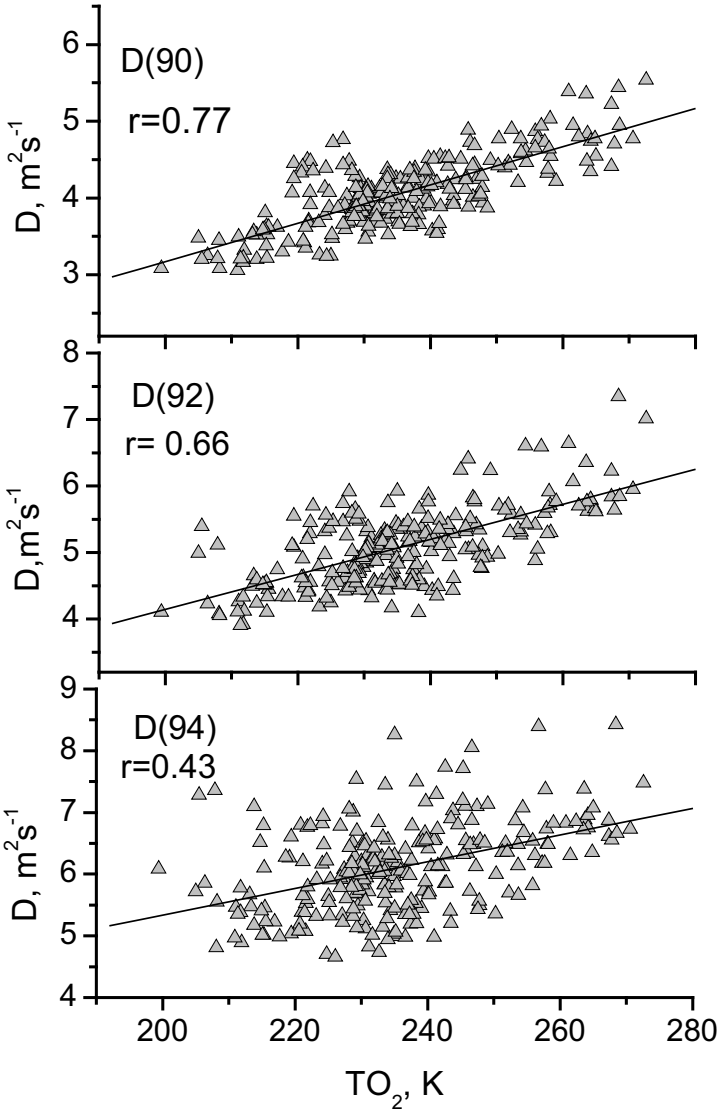

Fig. 3. Correlation between the O_2 rotational temperature and meteor trail ambipolar diffusion coefficient, D at 90 km (top), 92 km (middle) and 94 km (bottom). Each plot corresponds to a couple of D and TO_2 with half-hourly averaged values.

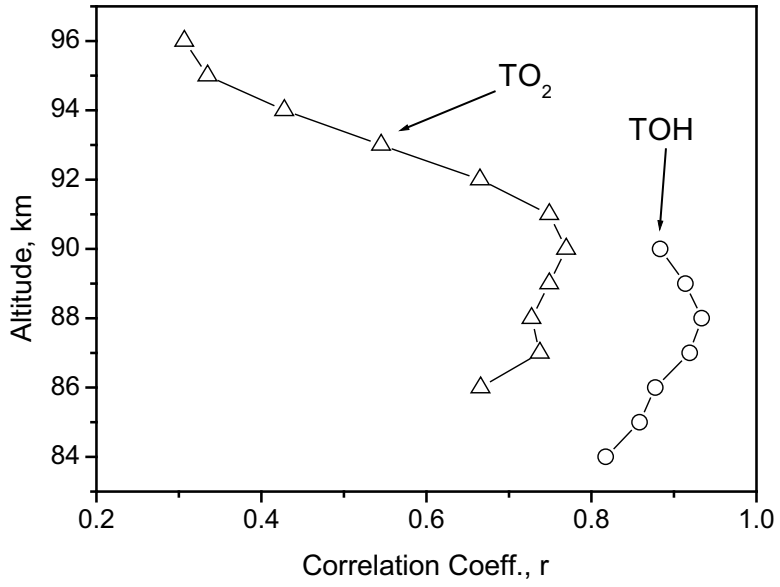

Fig. 4. Correlation coefficient between D and TO_2, and TOH as a function of altitude from 84 to 96 km. The TOH database is only for 6 nights in 2000.

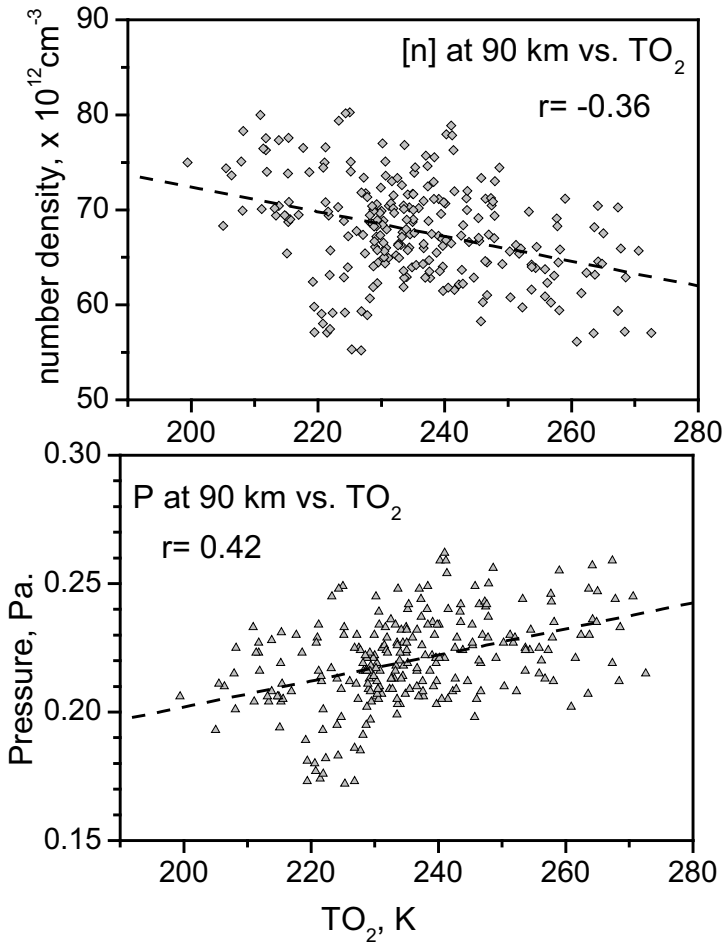

Fig. 5. Atmospheric number density, $[n]$, at 90 km versus O_2 rotational temperature, TO_2 (top), and the atmospheric pressure, P at 90 km, versus TO_2 (bottom).

aged values are shown. It is interesting to note that D values start to diffuse above 95 km. It could be due to large variability of the atmospheric temperature and density. Cervera and Reid (2000) pointed out the importance of interaction of the plasma trail with ambient magnetic field. According to them, the effect becomes important above 93 km. Further study would be necessary in order to explain it.

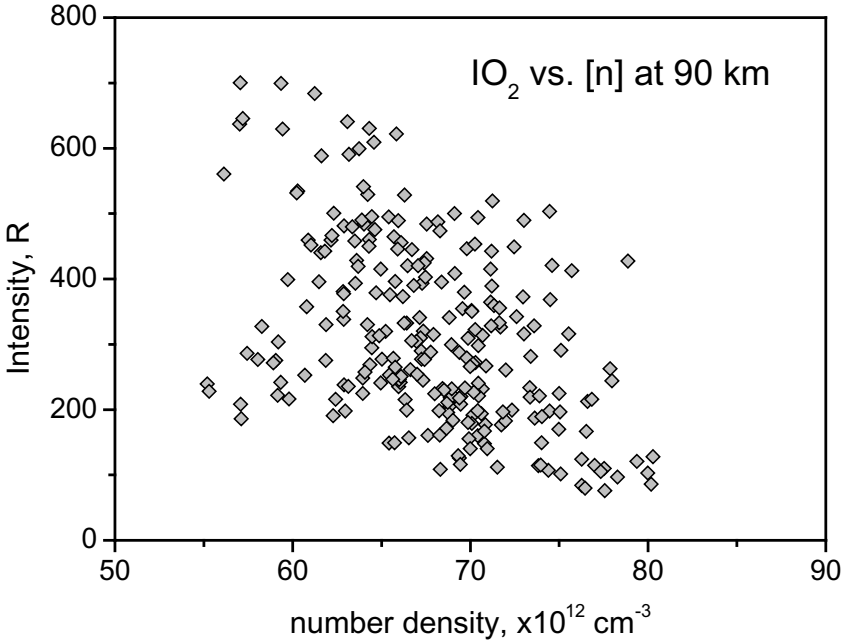

Fig. 6. O_2b(0,1) band intensity versus atmospheric number density at 90 km.

3.1 TO_2 vs. D at 90 km

Correlation study between the ambipolar diffusion coefficient, D, and TO_2 requires information on altitude of the O_2 emission layer, because D is strongly dependent on the atmospheric density, which is a function of height. From the rocket observations, it is believed that the emission layer peak height is located at around 94 km of altitude (Greer *et al.*, 1986). The layer, however, could change its height depending on the atomic oxygen profile and its recombination processes, $O + O + M \rightarrow O_2^* + M$, followed by $O_2^* + O_2 \rightarrow O_2(b)$. In order to check the unknown height, the (D, TO_2) values are plotted, for D at 90, 92 and 94 km in Fig. 3. It is clear to see that D and TO_2 are well correlated for D at 90 km. In order to check the correlation feature between TO_2 and D(z), the correlation coefficient was calculated choosing the D values from 86 to 96 km, and the results are shown in Fig. 4. It can be seen that D has a maximum correlation at 90 ± 1 km. This indicates that the O_2b emission height in this data set should be around 90 km, not 94 km as assumed previously based on rocket observations (Greer *et al.*, 1986). Also shown in the figure is in the case of TOH correlation with D from 84 to 90 km. The maximum correlation can be seen at 88 ± 1 km. This is very close to rocket observation data published elsewhere (Baker and Stair, 1988).

As mentioned in the previous section, the ambipolar diffusion coefficient D is a function of the local atmosphere temperature and density. For short period variations (1–6 hours) the density and temperature are not necessarily varying in phase. The half-hourly values ($D(z, t)$, $TO_2(t)$) therefore could include a phase lag effect. Therefore, nocturnal mean values ($D(z)$, $T(O_2)$) for the different altitudes are also compared, and found that the correlation coefficients again showed the highest for the group of D at 90 km.

3.2 [n] and P vs. TO_2

Using the D values at 90 km, the number density (cm^{-3}) and pressure (Pa) were calculated and are shown in Fig. 5. The density varied from 5.5 to 8.0×10^{13} cm^{-3}, and the pressure was between 0.18 and 0.25 Pa. These values are in agreement with MSISE-90 model atmosphere. The model shows, for example, the number density at 90 km at Shigaraki (35°N) varying from 6.0 to 7.6×10^{13} cm^{-3}, depending on the season. The number density shows a tendency of negative correlation with TO_2, while the pressure shows a positive correlation form, although both of them have a low level of correlation.

3.3 O_2 emission rates vs. [n]

The O_2b band emission rates and the number density [n] are plotted in Fig. 6. A negative correlation feature is noticeable. The relation between the OH emission rates and [n] presented by Takahashi *et al.* (2002) was also similar to the present result. Since both the emission rates are sensitive to the atmospheric density in the emission layer, the present result needs to be explained by some other factors.

4. Discussion

4.1 Why is the correlation of TO_2 with D optimum at 90 km

The best correlation of the O_2 temperatures with the meteor ambipolar diffusion coefficient D at 90 km altitude somewhat contradicts our knowledge of the O_2 emission height. Based on the rocket observations which have been carried out hitherto it is well known that the emission layer is located around 94 km of altitude with a half width of 8 km (Witt *et al.*, 1979; Greer *et al.*, 1986; Watanabe *et al.*, 1981; Takahashi *et al.*, 1996). Some rocket observations reported a lower peak height below 90 km (Witt *et al.*, 1984), but not as a common case. Therefore the difference of 4 km between the present result and the rocket observation is significant. The observed TO_2 temperature might not be necessarily representing a temperature at the emission peak height. If the temperature has a vertical gradient, positive during the summer and negative in winter, and the emission

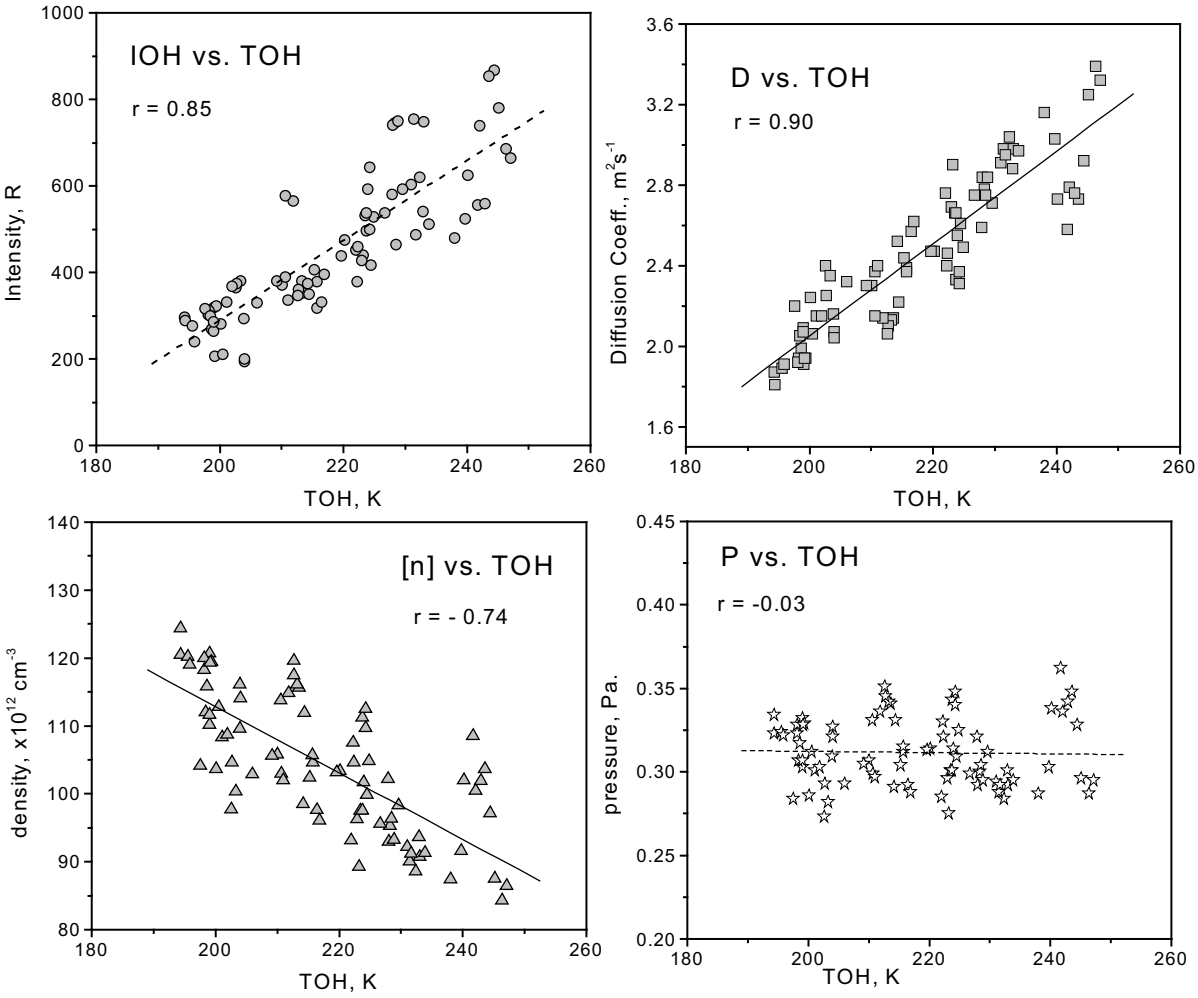

Fig. 7. Correlation between the OH(6,2) band intensity, TOH, D at 87 km, inferred atmospheric density, [n], and pressure, P. Database: see Table 2.

profile is not symmetric but in a form of Chapman layer, the brightness-weighted temperature TO_2 will tend to dislocate from the emission peak height. From the previous rocket measurements, however, the O_2b emission profile is known to be almost symmetric around the peak height (Greer *et al.*, 1986). Therefore the systematic displacement expected from this ambiguity should not be large as much as 4 km, the difference observed in the present study.

The O_2 emission peak height is dependent on photochemical balance of the atomic oxygen concentration, temperature and density profiles between 80 and 100 km as mentioned before. Therefore it could change from day to day, even during the night when the tidal and gravity wave oscillations pass through the emission layer. Zhang and Shepherd (1999) reported, from the UARS satellite data, that the O(^{1}S) and OH emission heights dislocate as much as 2 km during the night by tidal oscillation of the atmosphere in the upper mesosphere region. In order to check the correlation of TO_2 and D for individual night, we also calculated the correlation coefficient of the nocturnal variations for each night again varying D from 88 to 96 km. The result was similar to that shown in Fig. 4. From the total of 18 nights, 9 nights showed the best correlation with D at 90 km, 3 nights with D at 92 km and 4 nights with D at 94 km. Only one night showed the best correlation with D at 96 km. It indicates that the O_2 emission height changes from night to night, varying from 90 to 96 km, and is frequently located at around 90 to 92 km. It should be remembered that our present data are concentrated during the winter season (November to December). No data was available from the summer months. Therefore the present results do not conclude that the O_2 emission layer is always located at around 90 to 92 km. The emission layer could be higher during the other seasons as the rocket observation reported. The OH data in 2000 showed the best correlation pattern at 88 km (Fig. 4). This is a good agreement with rocket measurements of the OH emission, 87 $\pm$ 3 km (Baker and Stair, 1988).

4.2 Anti-correlation of T and [n]

The estimated atmospheric density, [n], is anti-correlated with TO_2 (Fig. 5). A similar result has been reported by Takahashi *et al.* (2002) using the OH rotational temperature, TOH, measured by MULTI-4 photometer, and D at 87 km observed at the same place but in the other period. In the present study OH emission data were also available from the SATI spectrometer. Because of some ambiguity in absolute values of the SATI OH temperature data in 2000 (Shiokawa, private communication), the SATI rotational temperatures were normalized to those obtained by MULTI-4 photometer operated during the same period. The number density and pressure were calculated assuming that the OH

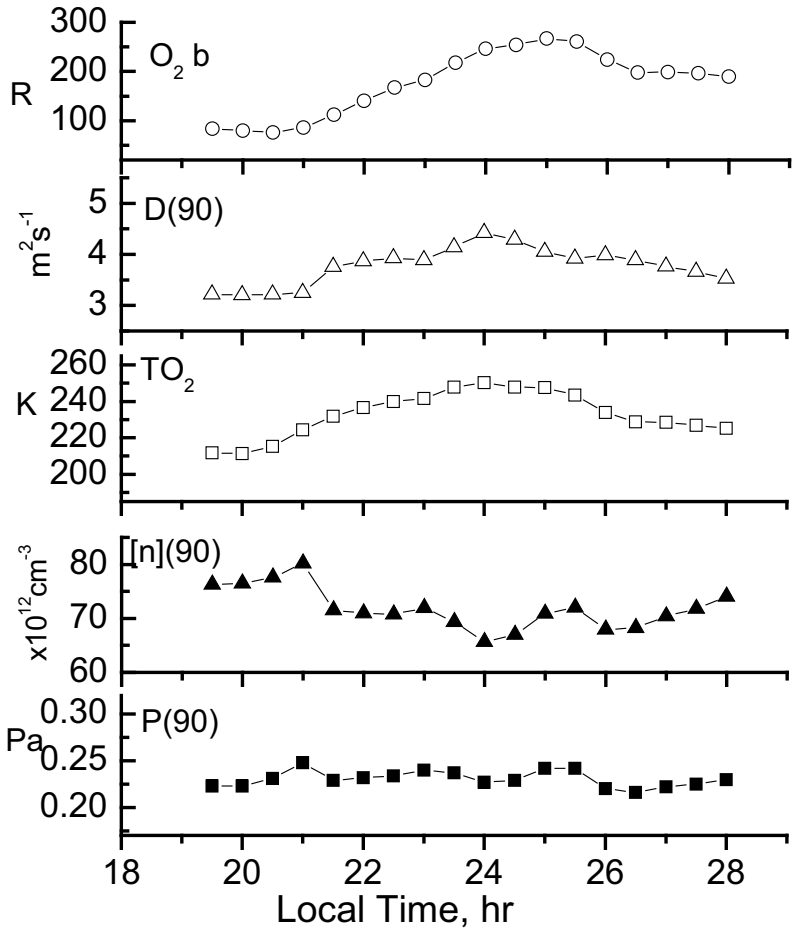

Fig. 8. Nocturnal variations of the O_2b(0,1) band intensity and temperatures, meteor radar D, and inferred density and pressure at 90 km altitude at Shigaraki on the night of December 22, 2000.

emission layer is located at around 87 km. The results are shown in Fig. 7. For the present analysis, only the OH data in 2000 (Table 2) were used. The correlation features are similar to those reported by Takahashi *et al.* (2002), with positive correlation between D and TOH. The inferred density [n] is again anti-correlated to TOH. The pressure, on the other hand, showed no variation with temperature. Therefore the anti-correlation between the temperature and density is a common feature in the mesopause region.

The anti-correlation between the atmospheric density and temperature can also be seen in the nocturnal variations. Figures 8 and 9 show nocturnal variations of the intensity and temperature of the O_2 and OH emissions, D, $[n]$ and pressure inferred from each emission, assuming that the emission height on this night was 87 km for OH and 90 km for the O_2 emissions. On this night, the airglow intensity and temperature for both the emissions increased toward midnight. Local time of the temperature maximum of TO_2 and TOH was shifted by 60 minutes, indicating that these variations were generated most probably by the tidal or inertial gravity wave oscillations, likely with the phase propagating downwards (Takahashi *et al.*, 1998). The temperature of TO_2 varied with an amplitude of 20 K (~8.7%). The atmospheric density at 87 and 90 km decreased to a minimum around midnight, opposite to the temperature variations. The amplitude of variation at 90 km was about 9%, approximately the same as the temperature. No wavelike oscillation was observed in the pressure variation.

The anti-correlation between the atmospheric density and temperature suggests that the atmosphere in the emission layers has a constant pressure variation under condition of Boussinesq approximation:

$$dT/T + dn/n = 0. \tag{8}$$

Our present results that the O_2 and OH emission rates have strong positive correlation with the local temperature variation and negative correlation with the density variation are difficult to understand straightforward. In the case of December 22 (Figs. 8 and 9), the increase of the temperature, about 35 K, from 20:00 LT to 24:00 LT, and the decrease of density, about 15% during the same period, could not explain the intensity increase of O_2b by a factor of 3 and a factor of 1.8 for the OH emission rates. If one considers that both the 3 body atomic oxygen recombination processes, O + O + M (responsible for production of an excited molecular oxygen) and O + O_2 + M (responsible for production of ozone and subsequently OH) have reaction rates which have a negative sense to the temperature variation (Campbell and Gray, 1973), these two emissions should decrease with increasing temperature. Some other processes (or factors) should be included in order to explain the strong increase. Vertical transport of atomic oxygen during the wave propa-

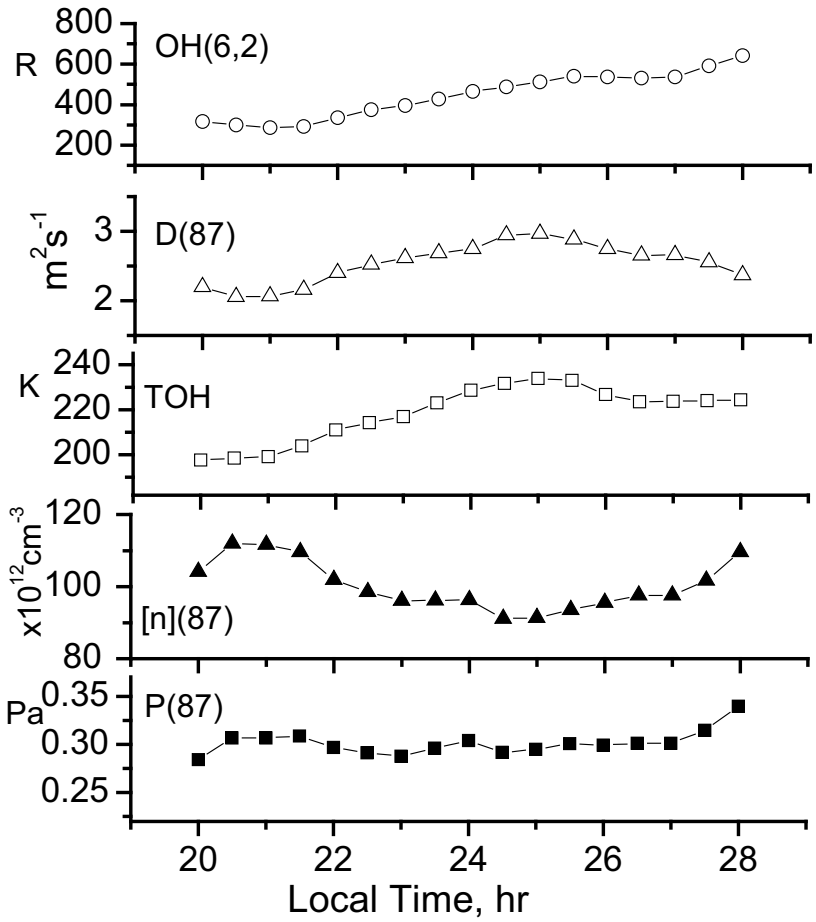

Fig. 9. Same as Fig. 8, except for OH(6,2) band intensity and temperature, density and pressure at 87 km height.

gating would be one such processes. Further model calculation of the emission rates considering more realistic model atmosphere should be necessary for further discussions.

5. Conclusions

Simultaneous measurement of the airglow O_2b(0,1) band temperature, TO_2, and meteor trail ambipolar diffusion coefficient, D, made it possible to infer atmospheric density, $[n]$ and pressure, P, in the emission layer. Good correlation between TO_2 and D was found for the D at around 90 km in height, suggesting that the O_2 emission layer is located at around 90 km, lower than believed from past rocket measurements. The inferred atmospheric densities, $[n]$, are anticorrelated to the temperature variation. This suggests that atmospheric perturbation, generated by tidal oscillation for example, would happen under a condition of constant pressure. Good positive correlation between the emission rates and temperature and negative correlation with the atmospheric density suggests that the emission rates are much more sensitive to the local temperature than the density. Present data are concentrated in the winter season. Further observation should be carried out for equinox and summer seasons in order to see further relationship between D and TO_2.

Acknowledgments. The MU radar belongs to and is operated by Radio Science Center for Space and atmosphere, RASC, Kyoto University. The SATI spectrometer belongs to and operated by Solar-Terrestrial Environment Laboratory, Nagoya University. Takahashi thanks CNPq (Brazilian National Research Council) for opportunity to work at Kyoto University under contract 201104/80-6.

References

Baker, D. J. and J. A. T. Stair, Rocket measurements of the altitude distributions of the hydroxyl airglow, *Physica Scripta,* **37**, 611–622, 1988.

Bittner, M., D. Offermann, H. H. Graef, M. Donner, K. Hamilton, An 18-year time series of OH temperatures and middle atmosphere decadal variations, *J. Atmos. Sol. Terr. Phys.*, **64**, 1147–1166, 2002.

Campbell, I. M. and C. N. Gray, Rate constants for O(3P) recombination and association with N(4S), *Chem. Phys. Lett.*, **8**, 259, 1973.

Cervera, M. A. and I. M. Reid, Comparison of atmospheric parameters derived from meteor observations with CIRA, *Radio Sci.*, **35**(3), 833–843, 2000.

Chilson, P. B., P. Czechowsky, and G. Schmidt, A comparison of ambipolar diffusion coefficients in meteor trains using VHF radar and UV lidar, *Geophys. Res. Letts.*, **23**(20), 2745–2748, 1996.

Greer, R. G. H., D. P. Murtagh, I. C. McDade, P. H. G. Dickinson, L. Thomas, D. B. Jenkins, J. Stegman, E. J. Llewellyn, G. Witt, D. J. Mackinnon, and E. R. Williams, Eton 1: A data base pertinent to the study of energy transfer in the oxygen nightglow, *Planet. Space Sci.*, **34**, 771–788, 1986.

Hocking, W. K., Temperatures using radar-meteor decay times, *Geophys. Res. Letts.*, **26**(21), 3297–3300, 1999.

Hocking, W. K., T. Thayaparan, and J. Jones, Meteor decay times and their use in determining a diagnostic mesospheric temperature-pressure parameter: methodology and one year of data, *Geophys. Res. Letts.*, **24**(23), 2977–2980, 1997.

Jones, W., The decay of radar echoes from meteors with particular reference to their use in the determination of temperature fluctuations near the mesopause, *Ann. Geophysicae,* **13**, 1104–1106, 1995.

Makhlouf, U. B., R. H. Picard, and J. R. Winick, Photochemical-dynamical

modeling of the measured response of airglow to gravity waves, *J. Geophys. Res.*, **100**(D6), 11289–11311, 1995.

Makhlouf, U. B., R. H. Picard, J. R. Winick, and T. F. Tuan, A model for the response of the atomic oxygen 557.7 nm and the OH Meinel airglow to atmospheric gravity waves in a realistic atmosphere, *J. Geophys. Res.*, **103**(D6), 6261–6269, 1998.

Meinel, A. B., OH emission bands in the spectrum of the night sky. I, *Trans. Amer. Geophys. Union,* **31**, 21, 1950.

Nakamura, T., T. Tsuda, M. Tsutsumi, K. Kita, T. Uehara, S. Kato, and S. Fukao, Meteor wind observations with the MU radar, *Radio Sci.*, **26**(4), 857–869, 1991.

Nakamura, T., T. Tsuda, S. Fukao, H. Takahashi, and R. A. Buriti, P. P. Batista, M. Tsutsumi, M. Ishii, K. Igarashi, H. Fukunishi, Y. Yamada, A. Nomura, T. D. Kawahara, K. Kobayashi, C. Nagasawa, M. Abo, and M. J. Taylor, Studies of the MLT regions using the MU radar and simultaneous observations with OH spectrometer and other optical instruments, *Adv. Space Res.*, **19**, 643–652, 1997.

Shiokawa, K., Y. Katoh, M. Satoh, M. K. Ejiri, T. Ogawa, T. Nakamura, T. Tsuda, and R. H. Wiens, Development of optical mesosphere thermosphere imagers (OMTI), *Earth Planets Space,* **51**, 887–896, 1999.

Takahashi, H., B. R. Clemesha, D. M. Simonich, S. M. L. Melo, N. R. Teixeira, A. Eras, J. Stegman, and G. Witt, Rocket measurements of the equatorial airglow: Multifot 92 data base, *J. Atmos. Terr. Phys.*, **58**(16), 1943–1961, 1996.

Takahashi, H., P. P. Batista, R. A. Buriti, D. Gobbi, T. Nakamura *et al.*, Simultaneous measurements of airglow OH emission and meteor wind by a scanning photometer and the MU radar, *J. Atmos. Solar Terr. Phys.*, **60**, 1649–1668, 1998.

Takahashi, H., T. Nakamura, T. Tsuda, R. A. Buriti, and D. Gobbi, First measurement of atmospheric density and pressure by meteor diffusion coefficient and airglow OH temperature in the mesopause region, *Geophys. Res. Letts.*, **29**(8), 1165/GL014101, 2002.

Tsutsumi, M., T. Tsuda, T. Nakamura, and S. fukao, Temperature fluctuations near the mesopause inferred from meteor observations with the middle and upper atmosphere radar, *Radio Sci.*, **29**(3), 599–610, 1994.

Watanabe, T., M. Nakamura, and T. Ogawa, Rocket measurements of O_2 atmospheric and OH Meinel bands in the airglow, *J. Geophys. Res.*, **86**, 5768–5774, 1981.

Wiens, R. H., S. P. Zhang, R. N. Peterson, and G. G. Shepherd, MORTI: A mesopause oxygen rotational temperature imager, *Planet. Space Sci.*, **39**, 1363–1375, 1991.

Wiens, R. H., A. Moise, S. Brown, S. Sargoytchev, R. N. Peterson, G. G. Shepherd, M. J. Lopez-Gonzalez, J. J. Lopez-Moreno, and R. Rodrigo, SATI: A spectral airglow temperature imager, *Adv. Space Res.*, **19**, 677–680, 1997.

Witt, G., J. Stegman, B. H. Solheim, and E. J. Llewellyn, A measurement of the O_2(b) atmospheric band and the OI(^{1}S) green line in the nightglow, *Planet. Space Sci.*, **27**, 341–350, 1979.

Witt, G., J. Stegman, D. O. Murtagh, I. C. McDade, R. G. H. Greer, P. H. G. Dickinson, and D. B. Jenkins, Collisional energy transfer and the excitation of O_2(b) in the atmosphere, *Journal of Photochemistry,* **25**, 365–378, 1984.

Yu, J. R. and C. Y. She, Climatology of a midlatitude mesopause region observed by a lidar at Fort Collins, Colorado (40.6N, 105W), *J. Geophys. Res.*, **100**(D4), 7441–7452, 1995.

Zhang, S. P. and G. G. Shepherd, The influence of the diurnal tide on the O(1S) and OH emission rates observed by WINDII on UARS, *Geophys. Res. Lett.*, **26**(4), 529–532, 1999.

Zhang, S. P., R. G. Roble, and G. G. Shepherd, Tidal influence on the oxygen and hydroxyl nightglows: Wind imaging interferometer observations and thermosphere/ionosphere/mesosphere electrodynamics general circulation model, *J. Geophys. Res.*, **106**(A10), 21381–21393, 2001.

H. Takahashi (e-mail: hisao@laser.inpe.br), T. Nakamura, K. Shiokawa, T. Tsuda, L. M. Lima, and D. Gobbi